Hyporheic flow under periodic bedforms influenced by low-density gradients

Guangqiu Jin[1,2,#], Hongwu Tang[1,2], Ling Li[3,1], D. A. Barry[4]

[1] State Key Laboratory of Hydrology-Water Resources and Hydraulic Engineering, Hohai University, Nanjing, China

Emails: jingq@hhu.edu.cn, hwtang@hhu.edu.cn

[2] Centre for Eco-Environment Modelling, The College of Water Conservancy and Hydropower Engineering, Hohai University, Nanjing, China

[3] National Centre for Groundwater Research and Training, School of Civil Engineering, The University of Queensland, Queensland, Australia

Email: l.li@uq.edu.au

[4] Laboratoire de technologie écologique, Institut d'ingénierie de l'environnement, Faculté de l'environnement naturel, architectural et construit (ENAC), Ecole Polytechnique Fédérale de Lausanne (EPFL), Station 2, 1015 Lausanne, Switzerland

Email: andrew.barry@epfl.ch

Resubmitted to *Geophysical Research Letters* on 22 September 2011

[#] Author to whom all correspondence should be addressed. Tel: +86 (25) 8378-6919. Fax: +86 (25) 8378-6919

Abstract

Small density variations across streambeds due to low solute concentrations in stream water exist commonly in streams and rivers. Using laboratory experiments and numerical modeling, we demonstrated that even small density variations can influence hyporheic flow in streambeds with periodic bedforms. The circulating pore water flow patterns in the bed were modified constantly as the solute front moved downward. Density-induced head gradients eventually overwhelmed the regional hydraulic gradient and drove the circulating flow below a hydraulic divide that would have existed without the density influence. The density-modified hyporheic flow provided a relatively fast solute transport mechanism and enhanced the overall mass exchange between the stream and bed. These results highlight the important role of weak, upward density gradients in modulating hyporheic flow.

Keywords: Water quality; solute transport; advection; hyporheic zone; mass flux

1. Introduction

Hyporheic flow induces significant solute exchange across streambeds, affecting water quality in both the stream and bed (Figure S1a) [*Hill et al.*, 1998; *Pretty et al.*, 2006]. Numerous investigations have been carried out to examine hyporheic flow and associated solute transport processes under the influences of stream water flow, stream network morphology and bedforms, sediment properties, and regional hydraulic gradients in the shallow aquifer [*Bencala et al.*, 1984; *Cardenas et al.*, 2004; *Salehin et al.*, 2004; *Boano et al.*, 2006; *Packman et al.*, 2006; *Cardenas*, 2008; *Revelli et al.*, 2008]. Many studies focused on hyporheic flow driven by hydraulic head gradients due to stream flow and bedform interactions (Figure S1b) [*Elliott and Brooks*, 1997; *Cardenas and Wilson*, 2007; *Jin et al*., 2010].

Laboratory experiments have been conducted to quantify the hyporheic exchange using salt or other solutes as the tracer [*Marion et al.*, 2003; *Salehin et al.*, 2004; *Jin et al.*, 2010]. The solutes in these experiments were typically released at low concentrations, a common condition that also exists in natural streams and rivers [*Boano et al.*, 2009]. The low solute concentrations led to only small density variations between the stream water and underlying pore water in the bed [*Boano et al.*, 2009]. Such small density variations have been assumed to have little effect on the hyporheic flow and solute transport, and hence have been largely neglected [*Marion et al.*, 2003; *Salehin et al.*, 2004; *Jin et al.*, 2010]. However, *Boano et al*. [2009] demonstrated that the weak density gradient due to low solute concentrations in the stream water was capable of driving significant hyporheic

53 exchange between a model stream and its flat streambed in a flume experiment. The flow
54 driven by the density gradient provided an advective solute transport mechanism,
55 overwhelming the diffusive transport.

56 The purpose of this study was to examine effects of low-density gradients on
57 hyporheic flow and solute transport processes in a streambed with periodic bedforms. In
58 contrast to a flat bed, a streambed with periodic bedforms is subjected to the influence of
59 relatively strong hydraulic head gradients generated by stream flow and bedform
60 interactions (Figure S1). The flow and associated solute transport driven by such gradients
61 dominate the hyporheic exchange processes and have been the focus of many previous
62 studies [*Elliott and Brooks*, 1997; *Salehin et al.*, 2004; *Jin et al.*, 2010]. The question
63 addressed here is whether the relatively weak density gradients impose modulating effects
64 on the hyporheic flow. We are particularly interested in how flow and solute transport
65 behave under the influence of density gradients in the deep area of the hyporheic zone
66 where a hydraulic divide would exist without the density effects due to the presence of an
67 underflow (Figure S1c). Previous studies have shown that, constrained by this hydraulic
68 divide, solute transport to the deeper area occurs slowly through diffusion/dispersion
69 [*Bottacin-Busolin and Marion*, 2010; *Jin et al.*, 2010]. Here we address the question of
70 whether density gradients induce flow and advective transport that enhances solute
71 transfer to the deeper area (Figure S1d).

72 To address this question, laboratory flume experiments similar to those of *Jin et al.*
73 [2010] were conducted with continuous measurements of solute concentrations in the

74 stream and pore water samples collected from two vertical arrays of sampling ports at
75 different depths (100-μl solution taken for each sample), located at the stoss and lee slopes
76 of a bedform (Figure S1c). These measurements allowed assessment of density effects on
77 the downward movement of the solute front. In simulating the experiments, we employed
78 both constant-density and variable-density models. Comparison between predictions of
79 these two models and the experimental data enabled the discernment of density effects on
80 the hyporheic flow and solute transport processes.

81 **2. Laboratory experiments and numerical simulations**

82 The experimental set-up follows that of *Jin et al*. [2010] based on a circulating
83 flume system. To avoid possible initial contamination of the pore water by residual
84 materials in the sediment prior to the experiment, artificial sand supplied by Nanjing
85 Ninglei Sand and Stone Factory (China) was used for the streambed. Our previous
86 experiments conducted with river sand did not reveal properly the density effect [*Jin et al*.,
87 2010]; we suspect that residual materials in the river sand used might have raised the
88 initial density of pore water, reducing the density contrast between the stream water and
89 pore water to a minor level in the experiment. The artificial sand used for the present
90 experiment was sieved between 30 mesh (D_1 = 0.60 mm) and 60 mesh sieves (D_2 = 0.25
91 mm), and made of 99% pure silicon dioxide. The bulk porosity was measured to be 0.46
92 using the water evaporation method. The saturated hydraulic conductivity, measured using
93 the constant-head method [*Chinese National Standard*, 1999], was found to be around

94 4.35×10^{-3} m s^{-1}. The sand was thoroughly cleaned before all experiments following the
95 method described by *Jin et al*. [2010]. The average flow velocity, water depth and pH in
96 the stream water were 12.26 cm s^{-1}, 10.21 cm and ~6.8, respectively. The experiment
97 started with freshwater in the streambed and a relatively low initial solute concentration
98 (1.73 kg m^{-3}) in the stream water. As the exchange between the stream and bed took place,
99 the solute concentration in the stream water decreased but remained spatially uniform due
100 to mixing through the flume circulation system [*Jin et al*., 2010].

101 A one-way sequential coupling method was used to simulate the stream water flow,
102 and pore water flow and solute transport in the streambed. First, the stream water flow
103 was computed using the CFD package FLUENT based on the Reynolds-averaged
104 Navier-Stokes equations together with the *k-ω* turbulence closure scheme [*Jin et al.*,
105 2010]. The predicted pressure at the sediment-water interface was then input into a
106 COMSOL-based model as boundary conditions to drive coupled pore water flow and
107 solute transport in the streambed [*Jin et al.*, 2010].

108 Density-dependent fluid flow in the bed is governed by [*COMSOL*, 2006]:

109 $$\rho S \frac{\partial h_f}{\partial t} + \theta \frac{\partial \rho}{\partial C} \frac{\partial C}{\partial t} + \nabla \cdot \left[-\rho K \left(\nabla h_f + \frac{\rho - \rho_f}{\rho_f} \nabla D_v \right) \right] = 0, \qquad (1)$$

110 where h_f (m), the equivalent freshwater hydraulic head, is given by $p/\rho g + D_v$ with p （Pa）
111 being the pore water pressure and D_v (m) the vertical coordinate directing upward; C (kg
112 m^{-3}) is the solute concentration; ρ (kg m^{-3}) is the fluid density; ρ_f (1000 kg m^{-3}) is the
113 freshwater density; S (m^{-1}) is the equivalent freshwater specific storativity, representing

114 storage due to compressibility of the fluid and porous medium [*Bear*, 1972]; t (s) is the
115 time; θ is the porosity; and K ($\mathrm{m\,s^{-1}}$) is the equivalent freshwater hydraulic conductivity.
116 The density of the fluid as a function of concentration is given by:

117 $$\rho = \rho_f + \frac{\partial \rho}{\partial C} C = \rho_f + \gamma C, \tag{2}$$

118 where γ is 0.7143 for the salt solution applied in the experiments [*Langevin et al.*, 2003].

119 The second term on the left hand side of equation (1) represents change in storage
120 due to concentration variations and is likely to dominate the compressible storage term
121 due to the relatively small compressibility of the artificial sand used in the study [*Bear*,
122 1972]. Coupled with the pore water flow, the salt solute transport in the porous bed is
123 governed by the conservative transport equation (e.g., *Jin et al*., 2010).

124 The initial and boundary conditions for both the stream flow model, and pore water
125 flow and solute transport model were essentially the same as those used by *Jin et al*.
126 [2010], simulating the conditions in the laboratory experiment. The predicted hydraulic
127 heads at the sediment-water interface from the stream flow simulation were converted to
128 the equivalent freshwater head based on the density of the stream water before its
129 application to define the boundary condition at the top of the bed for the pore water flow
130 simulation. Since the solute concentration and hence the density of the stream water
131 change with time as a result of solute exchange across the sediment-water interface, the
132 converted equivalent freshwater head prescribed at the interface varied temporally.
133 Periodic boundary conditions were applied to the lateral (vertical) boundaries for velocity,

134 pressure, concentration and solute flux. A no flow condition was applied at the bottom
135 boundary [*Jin et al.*, 2010]. The initial solute concentration in the pore water of the bed
136 was zero and a relatively low initial solute concentration (C_0= 1.73 kg m^{-3}) set for the
137 stream water.

138 **3 Results and discussion**

139 **3.1 Simulation cases**

140 A large number of simulations were conducted to examine the density effects on the
141 hyporheic flow and solute transport, in comparison with the experimental results. These
142 simulations covered cases (Table S1) with and without density effects, and with measured
143 and adjusted values of key model parameters (θ, K). The aim of the simulations was to
144 ascertain the effect of density gradients on hyporheic flow and solute transport, i.e.,
145 whether the density effects are essential for the model to predict the experimental results
146 or whether adjustment of the θ and K values is sufficient. Details of the results and
147 discussions for all the cases can be found in the supplementary materials. Here the focus
148 is on the first four cases:

149 Case 1: Neglecting density variations and using the measured hydraulic conductivity (K
150 $= 4.35 \times 10^{-3}$);

151 Case 2: Neglecting density variations and using an adjusted K ($= 21.8 \times 10^{-3}$ m s^{-1});

152 Case 3: Including density variations and using the measured K; and

153 Case 4: Including density variations and using an adjusted K ($=2.5 \times 10^{-3}$ m s^{-1}).

These cases took into account uncertainty in the measurements of the sediment properties, in particular, hydraulic conductivity, and hence allowed more rigorous assessment of density effects. The results are plotted in Figures 1-3 and S2 where comparison between the data and model predictions for the different cases can be made with regard to solute concentration in the stream water, and flow and solute transport in the bed.

3.2 Density effects on hyporheic flow dynamics, solute transport and exchange across the interface

A distinctive feature of the simulated density-dependent hyporheic flow is the temporal variations of the flow, which are linked to the downward movement of the solute front (case 4, Figure 3; and case 3, Figure S2). This is in contrast to the steady state condition of the simulated constant-density flow (i.e., without the density influence), in particular, the existence of a hydraulic divide separating the upper and lower flow zones throughout the simulation (case 1, Figure 3; and case 2, Figure S2). This hydraulic divide is due to an underflow caused by a pressure/head drop along the flume, as explained in previous studies [*Cardenas and Wilson*, 2007; *Jin et al*., 2010]. The fundamental difference between the variable- and constant-density flows has ramifications for solute transport in the streambed and exchange across the sediment-water interface.

As shown in Figure 1, the solute concentration in the overlying stream water decreased with time as the solute was transported into the bed. The concentration reduction at the beginning of the flume experiment and simulations (0-100 min) was rapid,

corresponding to the initial fast transfer of solute from the overlying water to the shallow streambed area, where the pore water flow velocity was relatively large mainly under the influence of hydraulic head gradients at the sediment-water interface. The flow in the shallow area was less affected by the density/concentration variations (26 and 180 min, Figure 3). Thus, all models with and without the density effect predicted similarly well the initial decrease of the solute concentration in the stream water (Figure 1).

The further reduction of the stream water solute concentration in the second phase (100-1100 min, Figure 1) was more gradual. During this stage, solute transport continued downward towards the deep area of the bed. The density gradient due to the concentration variation started to affect the flow as simulated in case 4 (Figure 3). This resulted in a considerable increase of the flow rate and significant changes in the flow pattern. After an elapsed time of 400 min, the circulation initiated from the sediment-water interface extended to the bottom boundary of the bed. This is in contrast with the separation of the upper and lower flow zones in the constant-density flow simulations (case 1, Figure 3; and case 2, Figure S2). The density effects on the flow led to a more rapid solute transfer to the deep area, particularly in the area close to the bottom boundary of the bed. Again, this bottom area would be separated from the upper circulating zones if the density effect was not considered as in cases 1 and 2 where the solute transfer across the hydraulic divide to the bottom area was due to solute diffusion – a very slow process. These manifestations of the effects of density on hyporheic flow are evident in the experimental results.

The density effects enhanced solute exchange across the sediment-water interface,

195 which led to a relatively rapid decrease of solute concentration in the stream water.
196 Without such effects taken into account, the constant-density flow and solute transport
197 model failed to reproduce the rapid solute concentration change observed in the laboratory
198 experiment (case 1 in Figure 1). More importantly, the constant-density model, unable to
199 provide a relatively fast, advective transport mechanism for the bottom area of the bed,
200 would not predict an asymptotic concentration, which was evident in the experiment over
201 a relatively short period. This asymptotic concentration represents a steady state condition
202 with no net exchange between the overlying stream water and pore water in the bed. In
203 this condition, the solute concentrations in both waters become the same, equal to
204 $C_0 V_s /(V_s + V_p)$ [*Jin et al.*, 2010], where V_s is total volume of water in the flume system
205 excluding pore water and V_p is the total volume of the pore water in the streambed. The
206 experimental results show that the concentration in the stream water reached a relatively
207 steady level after an elapsed time of 1300 min. Even with a five-fold increased hydraulic
208 conductivity, the model without the density effects included still failed to predict the
209 approach of the asymptotic state despite over-prediction of the earlier decrease of the
210 solute concentration (case 2 in Figure 1).

211 With the density effects included, the variable-density model was able to replicate the
212 observations from the experiment. Although adjustment of the hydraulic conductivity
213 from the measured value (4.35×10^{-3} m s^{-1}) to 2.5×10^{-3} m s^{-1} was necessary for the
214 model predictions to match the experimental results (case 4, Figure 1), the prediction of
215 the asymptotic condition (including case 3) indicated the important role played by the

density-driven flow in hyporheic exchange. The adjustment by a factor less than 2 is likely to be within the range of uncertainty with the hydraulic conductivity measurement.

Further evidence of the density effects on the hyporheic flow and solute transport is provided by the measurements of the pore water solute concentrations at the two arrays of sampling points (Figure 2). Again, without the density effect included, the constant-density model was unable to predict the downward movement of the solute front as shown by the measured concentration profiles. With no adjustment of the hydraulic conductivity, the model under-predicted the solute front movement except for the early time when the front was near the sediment-water face and the density effect was relatively insignificant. The model failed to predict the movement of the solute through into the bottom area of the bed (> 575 min in Figure 2) even with a five-fold increased hydraulic conductivity and at the cost of over-predictions for early times. As discussed above, this failure is due to the confinement of the upper circulations by the hydraulic divide, which persists in the constant-density flow simulation. In contrast, the variable-density model, with density effects accounted for, simulated the behavior of the solute front as observed in the experiment, especially in the area near the bottom of the bed.

4. Concluding remarks

Small density variations between the stream water and pore water in the streambed exist commonly in natural streams. Such variations also occur in laboratory experiments on hyporheic exchange, which typically release solutes to the stream water at low

236 concentrations as tracers for studying the hyporheic exchange processes. The effects of
237 small density variations on hyporheic flow and solute transport have been assumed to be
238 of little importance compared with other forcing factors such as hydraulic gradient due to
239 stream flow and bedform interactions. Using well-controlled laboratory experiments and
240 numerical simulations, we have demonstrated that even small density variations can
241 influence the hyporheic flow and solute transport in the streambed with the presence of
242 periodic bedforms.

243 The density effect leads to alteration of the flow rate and patterns as the solute front
244 moves downward. The main difference is that the density-induced head gradients drive the
245 circulating flow below a hydraulic divide that would exist without the density influence.
246 The modified hyporheic flows provide a relatively fast solute transport mechanism and
247 enhanced the overall mass exchange between the stream and bed. These findings will have
248 important implications for studies of river ecosystems including hyporheic zones.

249 The experimental set-up used here is one that has been adopted in many previous
250 studies [*Elliott and Brooks*, 1997; *Marion et al.*, 2003; *Boano et al.*, 2009; *Jin et al.*, 2010].
251 While the findings highlight the importance of small density variations as a driving factor
252 of hyporheic exchange processes, further investigation should be conducted to examine
253 the density effects on hyporheic flow and solute transport under different conditions such
254 as a pulse input of solute to the stream, large solute concentrations in the stream water and
255 downward density gradients (solutes initiated from the bed).

256 **Acknowledgments**

257 This research has been supported by the Natural Science Foundation of China
258 (50925932, 51109059), the Special Fund of State Key Laboratory of China (2011585612,
259 2011585112), the Natural Science Foundation of Hohai University (2009422211), the
260 Fundamental Research Funds for the Central Universities (2009B09514, 2010B21914)
261 and Australian Research Council (DP0988718). The authors acknowledge the assistance
262 provided by Xiaoquan Yang, Ming Chen and Kai Xie during the experiments.

263 **References**

264 Bear J. *Dynamics of fluids in porous media* (1972), Elsevier, New York, USA.

265 Bencala, K., V. Kennedy, G. Zellweger, A. Jackman, and R. Avanzino (1984), Interactions
266 of solutes and streambed sediment 1. An experimental analysis of cation and anion
267 transport in a mountain stream, *Water Resour. Res.*, *20*(12), 1797-1803,
268 doi:10.1029/WR020i012p01797.

269 Boano, F., C. Camporeale, R. Revelli, and L. Ridolfi (2006), Sinuosity-driven hyporheic
270 exchange in meandering rivers, *Geophys. Res. Lett.*, *33*(18), L18406,
271 doi:10.1029/2006GL027630

272 Boano, F., D. Poggi, R. Revelli, and L. Ridolfi (2009), Gravity-driven water exchange
273 between streams and hyporheic zones, *Geophys. Res. Lett.*, *36*(20), L20402,
274 doi:10.1029/2009GL040147.

275 Bottacin-Busolin, A., and A. Marion (2010), Combined role of advective pumping and

276 mechanical dispersion on time scales of bed form-induced hyporheic exchange,
277 *Water Resour. Res.*;*46*:W08518. doi:10.1029/2009WR008892.
278 Cardenas, M. B. (2008), Surface water-groundwater interface geomorphology leads to
279 scaling of residence times, *Geophys. Res. Lett.*, *35*(8), doi:10.1029/2008GL033753.
280 Cardenas, M. B., and J. L. Wilson (2007), Hydrodynamics of coupled flow above and
281 below a sediment-water interface with triangular bedforms, *Adv. Water Resour.*,
282 *30*(3), 301-313, doi:10.1016/j.advwatres.2006.06.009.
283 Cardenas, M. B., J. L. Wilson, and V. A. Zlotnik (2004), Impact of heterogeneity, bed
284 forms, and stream curvature on subchannel hyporheic exchange, *Water Resour. Res.*,
285 *40*(8), doi:10.1029/2004wr003008.
286 Chinese National Standard, (1999), *Standard for soil test methods*, GB/T50123-1999,
287 Beijing (in Chinese).
288 COMSOL (2006), *FEMLAB 3.3 Multiphysics Modeling - User's Guide*, COMSOL Inc.,
289 Burlington, Massachusetts, USA.
290 Elliott, A. H., and N. H. Brooks (1997), Transfer of nonsorbing solutes to a streambed
291 with bed forms: Laboratory experiments, *Water Resour. Res.*, *33*(1), 137-151.
292 Hill, A. R., C. F. Labadia, and K. Sanmugadas (1998), Hyporheic zone hydrology and
293 nitrogen dynamics in relation to the streambed topography of a N-rich stream,
294 *Biogeochemistry*, *42*(3), 285-310.
295 Jin, G., H. Tang, B. Gibbes, L. Li, and D. A. Barry (2010), Transport of nonsorbing solutes
296 in a streambed with periodic bedforms, *Adv. Water Resour*, *33*(11), 1402-1416,

297 doi:10.1016/j.advwatres.2010.09.003.
298 Langevin, C., W. Shoemaker, and W. Guo (2003), MODFLOW-2000, the US Geological
299 Survey modular ground-water model: Documentation of the SEAWAT-2000 version
300 with the variable-density flow process (VDF) and the integrated MT3DMS transport
301 process (IMT), *US Geological Survey Open-File Report*, *3*(426), 1-43.
302 Lin, H., D. Richards, C. Talbot, G.T. Yeh, H.P. Cheng and N.L. Jones (1997),
303 FEMWATER: A three-dimensional finite element computer model for simulating
304 density-dependent flow and transport in variably saturated media, Report
305 CHL-96-12, US Army Corps of Engineers, Vicksburg, MS.
306 Marion, A., M. Bellinello, I. Guymer, and A. Packman (2003), Effect of bed form
307 geometry on the penetration of nonreactive solutes into a stream bed, *Water Resour.*
308 *Res.*, *39*(1), doi:10.1029/2001WR000264.
309 Packman, A. I., A. Marion, M. Zaramella, C. Chen, J. F. Gaillard, and D. T. Keane (2006),
310 Development of layered sediment structure and its effects on pore water transport
311 and hyporheic exchange, *Water. Air. Soil Pollut.*, *6*(5), 69-78, doi:
312 10.1007/s11267-006-9057-y.
313 Pretty, J. L., A. G. Hildrew, and M. Trimmer (2006), Nutrient dynamics in relation to
314 surface-subsurface hydrological exchange in a groundwater fed chalk stream, *J.*
315 *Hydrol.*, *330*(1-2), 84-100, doi:10.1016/j.jhydrol.2006.04.013.
316 Revelli, R., F. Boano, C. Camporeale, and L. Ridolfi (2008), Intra-meander hyporheic
317 flow in alluvial rivers, *Water Resour. Res.*, *44*(12), doi:10.1029/2008WR007081.

318 Salehin, M., A. I. Packman, and M. Paradis (2004), Hyporheic exchange with
319 heterogeneous streambeds: Laboratory experiments and modeling, *Water Resour.*
320 *Res.*, *40*(11), doi:10.1029/2003WR002567.

321 **List of figures**

322 Figure 1. Comparison of experimental data and modeled solute concentrations in the
323 stream water. The solid horizontal line indicates the calculated steady state
324 concentration, $C_0V_s/(V_s+V_p)$. Hydraulic conductivity K ($\times$ 10^{-3} m s^{-1}) and
325 density effect (DE) in all figures below are the same as this figure.

326 Figure 2. Comparison between measured and predicted solute concentrations varying
327 with depth. The solid horizontal line indicates the location of the hydraulic
328 divide at sampling array N1 or N2 (locations of the sampling points are shown
329 in Figure S1c).

330 Figure 3. Comparison of modeled solute concentration distribution, flow velocity (white
331 arrows) and streamline (grey line) at different elapsed times for different cases
332 with and without density effects. The color scale represents solute
333 concentration (C) in the streambed, with warm colors for high concentration
334 and cool for low concentration. The thick grey line shows the hydraulic divide
335 predicted by the constant-density flow model. This divide is also shown in the
336 results of the variable-density model for comparison. The results from case 3
337 (shown in Figure S2) exhibit similar trends to those from case 4 except for
338 over-predictions of hyporheic flow and downward solute transfer.

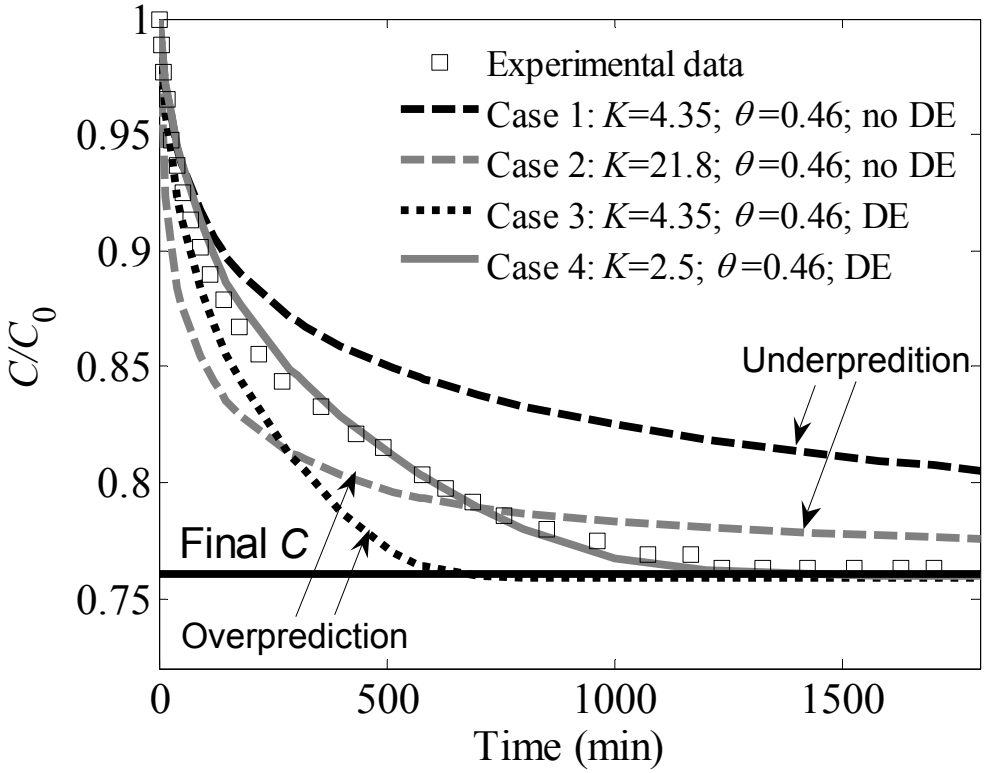

343

344 Figure 1

345

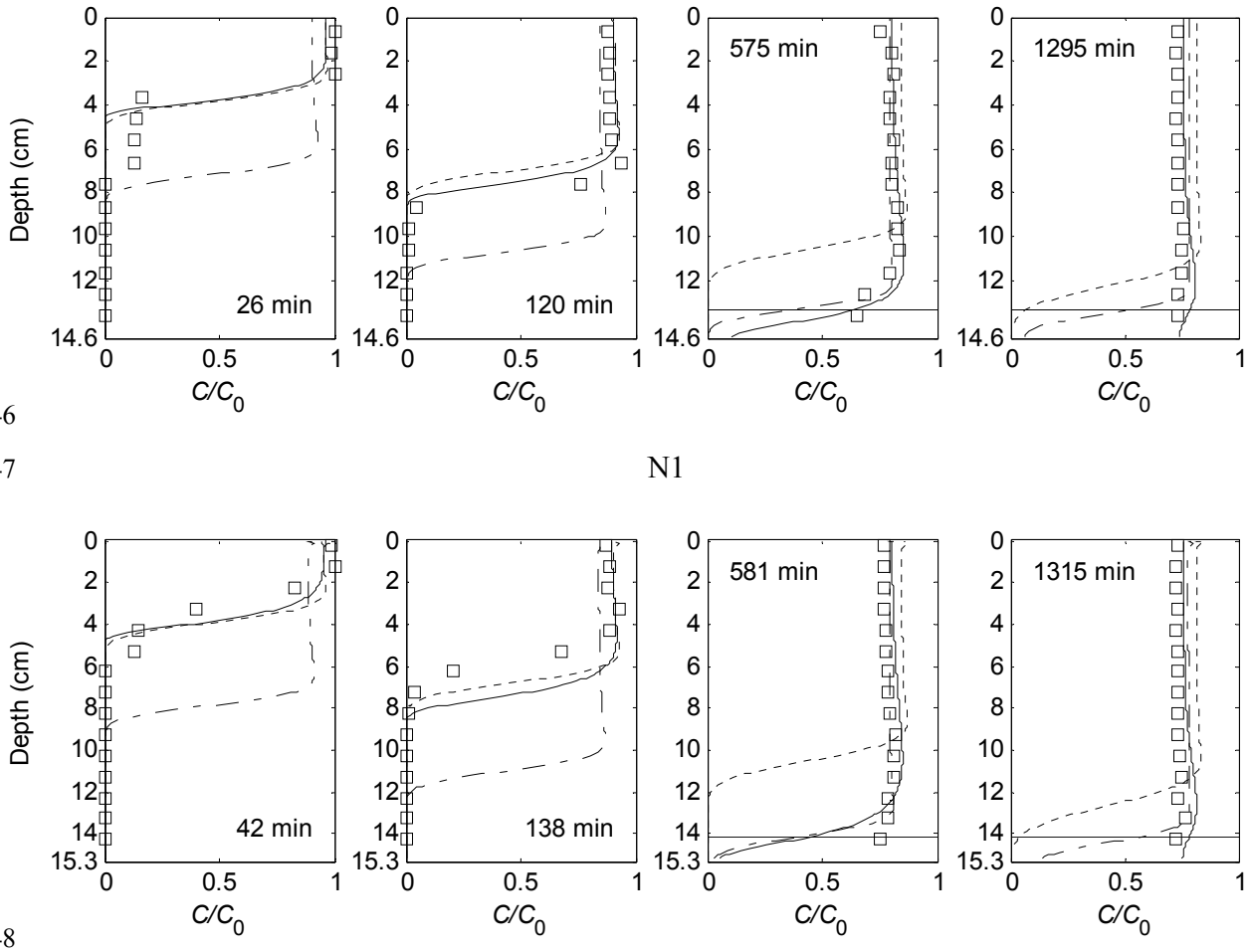

346

347

348

349

350

351 Figure 2

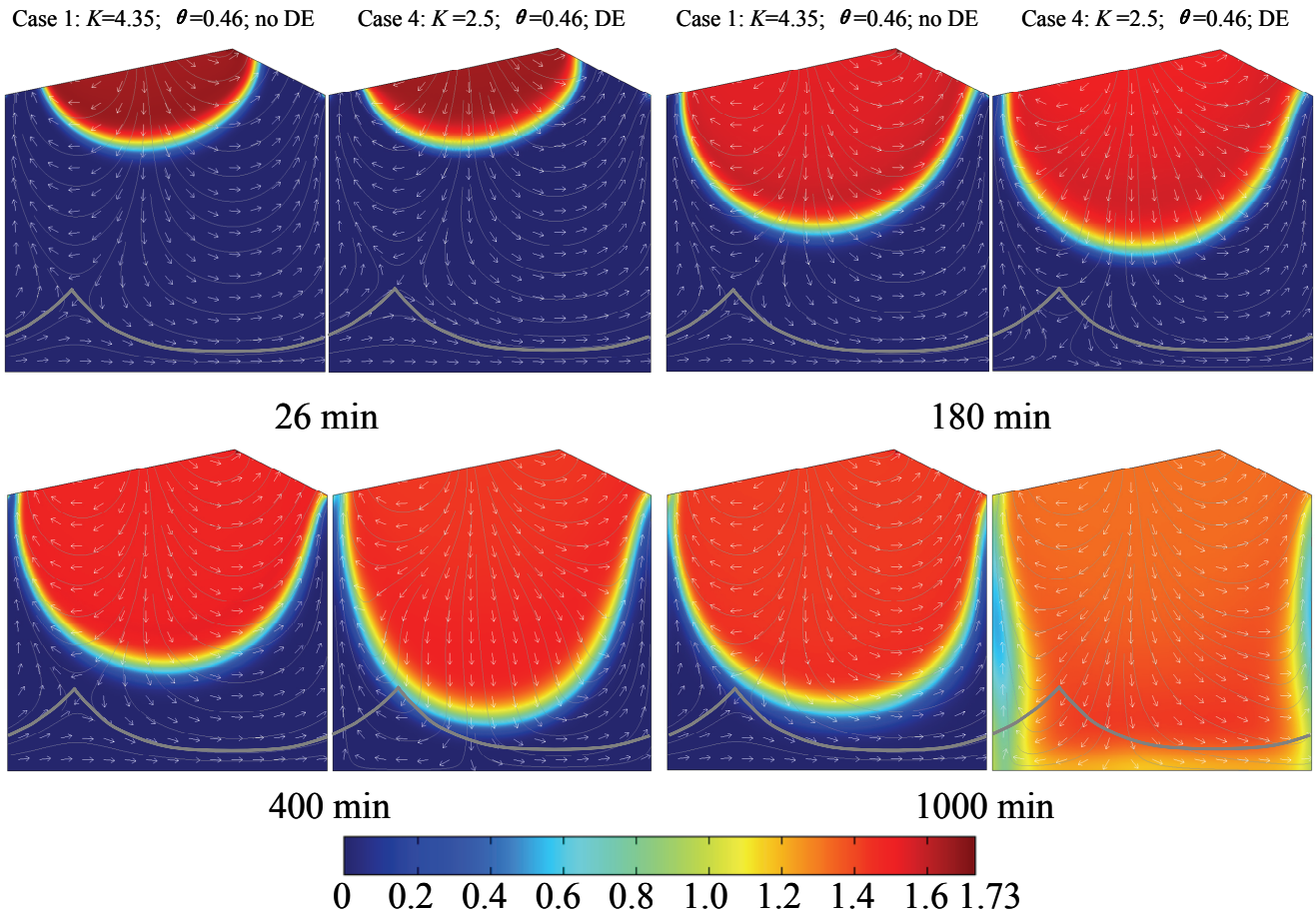
Case 1: K=4.35; θ=0.46; no DE
Case 4: K =2.5; θ=0.46; DE
Case 1: K=4.35; θ=0.46; no DE
Case 4: K =2.5; θ=0.46; DE
26 min
180 min
400 min
1000 min
0 0.2 0.4 0.6 0.8 1.0 1.2 1.4 1.6 1.73

Figure 3